

# Formation of a lamellar 14H-type long period stacking ordered structure in an as-cast Mg–Gd–Zn–Zr alloy

Y. J. Wu · D. L. Lin · X. Q. Zeng · L. M. Peng ·  
W. J. Ding

Received: 18 November 2008 / Accepted: 19 December 2008 / Published online: 27 January 2009  
© Springer Science+Business Media, LLC 2009

**Abstract** A novel as-cast  $\text{Mg}_{96.82}\text{Gd}_2\text{Zn}_1\text{Zr}_{0.18}$  alloy was produced by conventional ingot metallurgy. By scanning electron microscope and transmission electron microscope observations, its as-cast microstructure is mainly composed of the  $\alpha'$ -Mg solid solution, the coherent fine-lamellae and the eutectic. The  $\beta$ -phase ( $(\text{Mg,Zn})_3\text{Gd}$ ) as the second phase in eutectic has a face-center cubic structure. While, the coherent lamellae consist of the 2H–Mg and the 14H-type long period stacking ordered (LPSO) structure. At present, the lamellar 14H-type LPSO structure has first been observed within  $\alpha'$ -Mg matrix in the as-cast Mg–Gd–Zn–Zr alloys. It can be concluded that the lamellar 14H-type LPSO structure within  $\alpha'$ -Mg matrix is a special structure obviously different from  $\alpha$ -Mg matrix (2H-type structure) in structure, composition, and formation condition.

## Introduction

Due to lightweight, high-strength, high-creep resistance, and other excellent performances, magnesium alloys containing rare earth (RE) elements (especially heavy RE) have systematically been investigated and widely developed as promising materials [1–7] used in automobile, electronics, military, and aerospace industries etc. A certain amount of Zn addition can further improve strengthening response of Mg–RE alloys [2]. Thereby, Mg–RE–Zn alloys have gradually been focused on, due to solution strengthening and aging strengthening etc. [1, 2].

At present, long period stacking ordered (LPSO) structures have been focused on in Mg–RE–Zn (RE = Y, Dy, Ho, Er, Gd, Tb, Tm) alloys [8–24]. For example, in 2001, a high-strength  $\text{Mg}_{97}\text{Zn}_1\text{Y}_2$  (at.%) alloy produced by rapidly solidified powder metallurgy (RS/PM) exhibits remarkable mechanical properties with a tensile yield strength of 610 MPa and an elongation of 5% at room temperature [9]. With respect to types of the LPSO structures, there are 6H, 10H, 14H, 18R, 24R [8–24]. In these reports [8–22], based on if LPSO structure exists in as-cast alloys, Mg–RE–Zn (RE = Y, Dy, Ho, Er, Gd, Tb, Tm) alloys can be classified into two types. For type I, there are LPSO structures in as-cast alloys, including as-cast Mg–RE (RE = Y, Dy, Ho, Er, Tm)–Zn alloys [8–23]. While, for type II, there are no LPSO structures in as-cast alloys, but LPSO structures appear after annealing at high temperatures, including as-cast Mg–RE (RE = Gd, Tb)–Zn alloys [19–22]. In previous reports [20–22], LPSO structures have not been observed in as-cast Mg–Gd–Zn (–Zr) alloys such as  $\text{Mg}_{96.5}\text{Zn}_1\text{Gd}_{2.5}$  [20] and  $\text{Mg}_{97}\text{Zn}_1\text{Gd}_2$  [21, 22] alloys, which are classified as type II. However, in our recent studies, by conventional ingot metallurgy, the coherent lamellar 14H-type LPSO structure was first found within

---

Y. J. Wu · D. L. Lin (✉) · X. Q. Zeng · L. M. Peng ·  
W. J. Ding  
National Engineering Research Center of Light Alloy Net  
Forming, Shanghai Jiao Tong University,  
800 Dongchuan Road, 200240 Shanghai,  
People's Republic of China  
e-mail: dllin@sjtu.edu.cn

D. L. Lin  
School of Materials Science and Engineering,  
Shanghai Jiao Tong University,  
800 Dongchuan Road, 200240 Shanghai,  
People's Republic of China

Y. J. Wu · X. Q. Zeng · L. M. Peng · W. J. Ding  
The State Key Laboratory of Metal Matrix Composites,  
Shanghai Jiao Tong University, 800 Dongchuan Road,  
200240 Shanghai, People's Republic of China

$\alpha'$ -Mg matrix in an as-cast  $\text{Mg}_{96.82}\text{Gd}_2\text{Zn}_1\text{Zr}_{0.18}$  alloy during solidification. Thus, as-cast Mg–Gd–Zn (–Zr) alloy should be classified as type I. The observation may be important for further clarifying the formation mechanism of the LPSO structures in Mg–RE–Zn (–Zr) alloys.

This article reports microstructure of the as-cast  $\text{Mg}_{96.82}\text{Gd}_2\text{Zn}_1\text{Zr}_{0.18}$  alloy. Moreover, formation and characterization of the lamellar 14H-type LPSO structure within  $\alpha'$ -Mg matrix in as-cast Mg–Gd–Zn–Zr alloy are emphasized.

## Experimental procedures

The alloy studied in this study is  $\text{Mg}_{96.82}\text{Gd}_2\text{Zn}_1\text{Zr}_{0.18}$  (nominal composition, at.%). It was prepared from the pure (>99.95%) Mg, Zn, and Mg–25% Gd (wt%) and Mg–30% Zr (wt%), which were preheated to about 473 K. Pure Mg (>99.95%) was melted in an electric resistance furnace with a mild steel crucible under a protective mixed gas of  $\text{SF}_6$  (0.3 vol.%) and  $\text{CO}_2$  (99.7 vol.%). Pure Zn metal and Mg–25% Gd (wt%) were melted at about 973 K. Mg–30% Zr (wt%) was added into the melt at about 1,053 K. Finally, the melt was poured at about 1,013 K into a graphite-coated mild steel mold preheated to about 473 K. The alloy ingots were cooled in air, cut into small specimens.

The melting point and eutectic temperature of this alloy were studied via DTA1600-type differential thermal analysis (DTA) at a heating rate of 10 K/min. Microstructure etched with 4%  $\text{HNO}_3$  in ethanol was observed using a LEO1450 scanning electron microscope (SEM) at 10–20 kV equipped with an Oxford energy disperse X-ray spectrometer (EDS). The thin foil for transmission electron microscope (TEM) observations was thinned by twin-jet electro polishing in a solution of 5%  $\text{HClO}_4$  in ethanol under the conditions of 20 mA, 75 V, and 233 K and then by low energy beam ion thinning with an incidence angle of  $4^\circ$  and a voltage of 3.5 V for 0.5 h. Then, TEM observations were carried out using a JEOL-2010 operating at 200 kV equipped with EDS.

## Results and discussion

### Microstructure of the as-cast Mg–Gd–Zn–Zr alloy

Figure 1 shows DTA traces for the as-cast  $\text{Mg}_{96.82}\text{Gd}_2\text{Zn}_1\text{Zr}_{0.18}$  alloy. It is evident that its melting point and eutectic temperature are about 904 and 804 K, respectively.

Figure 2a and b show SEM micrographs of the as-cast  $\text{Mg}_{96.82}\text{Gd}_2\text{Zn}_1\text{Zr}_{0.18}$  alloy. With the melt temperature

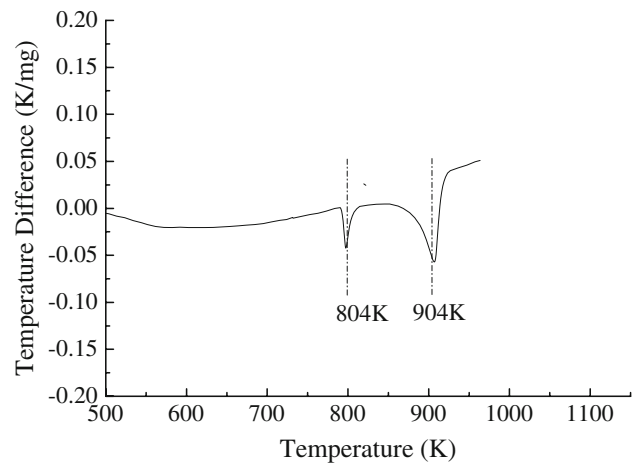


**Fig. 1** Differential thermal analysis traces of the as-cast  $\text{Mg}_{96.82}\text{Gd}_2\text{Zn}_1\text{Zr}_{0.18}$  alloy

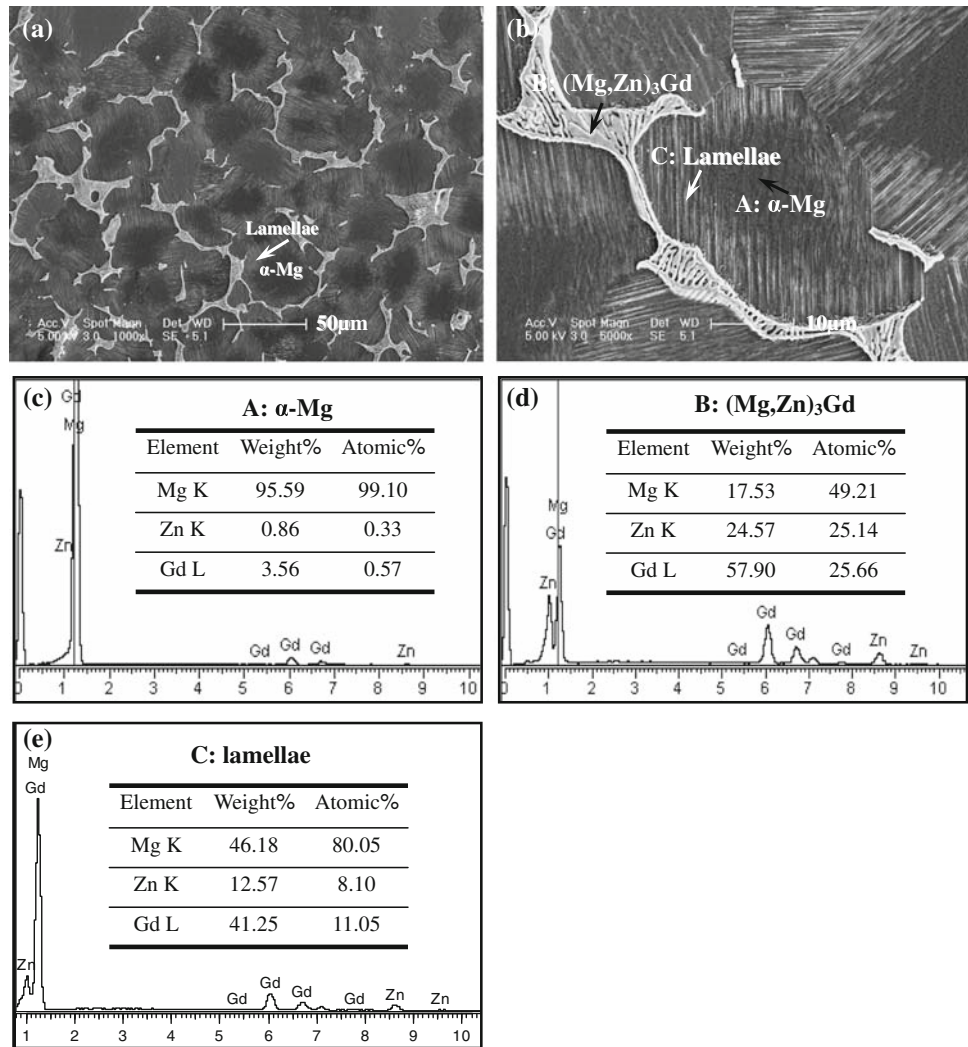
decreases from about 1,013 K,  $\alpha$ -Zr nuclei form first. Then, with the melt temperature decreases down to about 904 K, an  $\alpha$ -Mg phase nucleates on the  $\alpha$ -Zr particles to form an  $\alpha$ -Mg matrix (label A in Fig. 2b). The 0.18 at.% Zr can adequately refine  $\alpha$ -Mg matrix up to 31.9  $\mu\text{m}$ . Figure 2c shows the analysis of the EDS in the SEM mode of  $\alpha$ -Mg matrix. The result indicates that the average chemical compositions of the  $\alpha$ -Mg matrix is Mg–0.33  $\pm$  0.1 at.% Zn–0.57  $\pm$  0.1 at.% Gd.

During nucleation and growing of the  $\alpha$ -Mg matrix, with the melt temperature continuously decreases to about 804 K, a eutectic reaction occurs as follows  $\text{L} \xrightarrow{804\text{K}} \alpha\text{-Mg} + (\text{Mg,Zn})_3\text{Gd}$ . The dendritic eutectic structure can well be seen at grain boundaries as shown as label B in Fig. 2b. The eutectic is composed of an  $\alpha$ -Mg phase and a  $\beta$ -phase. The  $\beta$ -phase acts as a second phase in eutectic. By analysis of the EDS in the SEM mode (Fig. 2d), the composition of the  $\beta$ -phase was confirmed to be Mg–25.14  $\pm$  1.0 at.% Zn–25.66  $\pm$  1.0 at.% Gd. Therefore, the  $\beta$ -phase was estimated to be an  $(\text{Mg,Zn})_3\text{Gd}$  phase.

Figure 3 shows TEM observations for the  $\beta$ -phase in the as-cast  $\text{Mg}_{96.82}\text{Gd}_2\text{Zn}_1\text{Zr}_{0.18}$  alloy. Figure 3a, b, and c shows bright-field (BF) image and selected-area electron diffraction (SAED) patterns with the electron beam parallel to the [001] and [011] zones, respectively. The results indicate that the  $\beta$ -phase has a face-center cubic (fcc) structure with lattice constant of  $a = 0.719$  nm. Thereby, both as the second phase in the eutectic, the  $\beta$ -phase– $(\text{Mg,Zn})_3\text{Gd}$  with a fcc structure in this study is distinguished from the X-phase– $\text{Mg}_{12}\text{ZnY}$  with a 18R-type LPSO structure in as-cast Mg–Y–Zn alloys in terms of structure and composition [8, 14, 16, 19].

In addition, what's important is the coherent fine-lamellae were first observed within  $\alpha'$ -Mg matrix in as-cast

**Fig. 2** SEM micrographs of the as-cast  $Mg_{96.82}Gd_2Zn_1Zr_{0.18}$  alloy: **a** low magnification, **b** high magnification; **c–e** EDS spectra of (A)–(C) areas in (b)



Mg–Gd–Zn–Zr alloys. Formation and characterization analyses for the lamellae will be discussed in detail as follows.

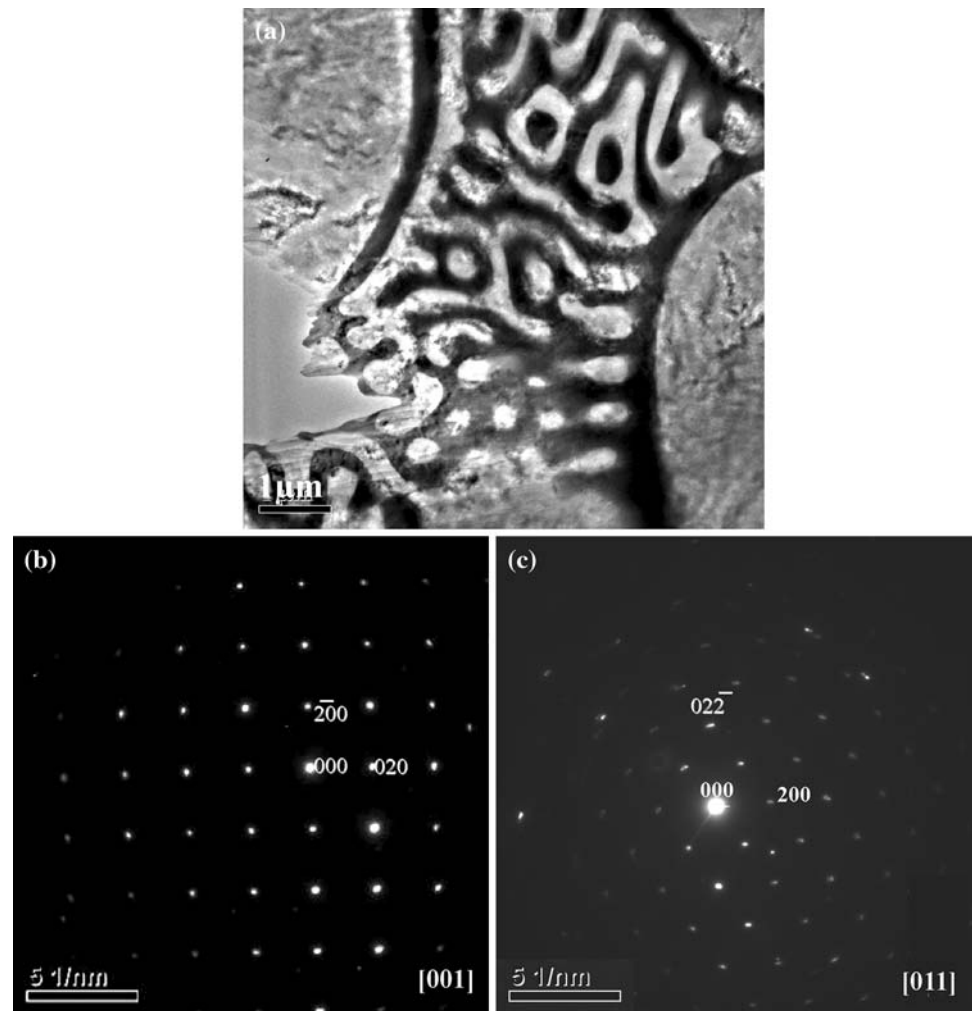
Formation of a 14H-type LPSO structure in as-cast Mg–Gd–Zn–Zr alloy

Interestingly, during cooling of the  $Mg_{96.82}Gd_2Zn_1Zr_{0.18}$  alloy ingot, modulations of Mg, Zn, and Gd atoms can result in these atoms deflecting normal lattice locations so that stacking faults (SFs) are formed. When interplanar distances generate periodical alterations, and composition order and stacking order for Zn and Gd atoms and other thermodynamic and dynamic requirements are all satisfied, the lamellae (white arrows in Fig. 2a and b and label C in Fig. 2b) are formed within  $\alpha'$ -Mg matrix. As shown in Fig. 2a and b, the lamellae are formed from grain boundaries to interiors because more Zn and Gd elements enrich in grain boundaries. While, not all the lamellae are formed breakthrough whole grains due to the limit of the formation

conditions controlled by composition order and stacking orders. At present, formation of the lamellae has first been found in as-cast Mg–Gd–Zn–Zr alloys.

Figure 4a–d show TEM observations for the morphology and structure of the lamellae. BF images and corresponding SAED pattern with the electron beam parallel to the  $[100]_z$  zone are shown in Fig. 4a–c and d, respectively. The results indicate that one of the lamellae, i.e., the  $\alpha$ -Mg matrix has a 2H-type hexagonal closed packed structure. While, the other has a 14H-type LPSO structure because there is 14 spots having almost equal distances between the center spot and the  $(002)_{Mg}$  spot. The 14H-type LPSO structure is formed along  $c^*$  axis  $\perp [001]$  of the 2H–Mg. In conclusion, the fine-lamellae consist of the 2H–Mg and the 14H-type LPSO structure. There is coherent relationship, i.e.,  $(001)_{2H-Mg} // (0014)_{14H-LPSO}$  and  $[001]_{2H-Mg} // [001]_{14H-LPSO}$ . In addition, the lattice constants of the 2H–Mg and the 14H-type LPSO structure are estimated to be  $a = 0.325$  nm,  $c = 0.520$  nm and  $a = 0.325$  nm,  $c = 3.722$  nm, respectively.

**Fig. 3** TEM observations for the  $\beta$ -phase in the as-cast  $\text{Mg}_{96.82}\text{Gd}_2\text{Zn}_1\text{Zr}_{0.18}$  alloy: **a** bright-field (BF) image; **b** and **c** selected-area electron diffraction (SAED) patterns with the electron beam parallel to the [001] and [011] zones, respectively



Furthermore, by analysis of the EDS in the SEM mode (Fig. 2e), the average chemical compositions of the 14H-type LPSO structure (label C in Fig. 2b) is  $\text{Mg}-8.10 \pm 1.0 \text{ at.}\% \text{ Zn}-11.05 \pm 1.0 \text{ at.}\% \text{ Gd}$ . In this study, more Gd and Zn atoms enrich the lamellar 14H-type LPSO structure as compared with the 2H-Mg. Thus, it can be concluded that the lamellar 14H-type LPSO structure within  $\alpha'$ -Mg matrix is a special structure obviously different from  $\alpha$ -Mg matrix (2H-type structure) in structure, composition, and formation conditions.

Since the 14H-type LPSO structure is composition order and stacking order, it is impossible for Gd and Zn atoms to uniformly distribute in its 14 atomic layers but their enrichment is periodical in its two atomic layers. So, the differences in SF energy and composition within the 14H-type LPSO structure result in the periodical differences in contrasts as well shown in Fig. 4c.

At present, formation of the lamellar 14H-type LPSO structure in the as-cast Mg-Gd-Zn (-Zr) alloys have not been observed in these reports [1, 20–22, 25]. In reported  $\text{Mg}_{96.5}\text{Zn}_1\text{Gd}_{2.5}$  [20] and  $\text{Mg}_{97}\text{Zn}_1\text{Gd}_2$  [21, 22], there are

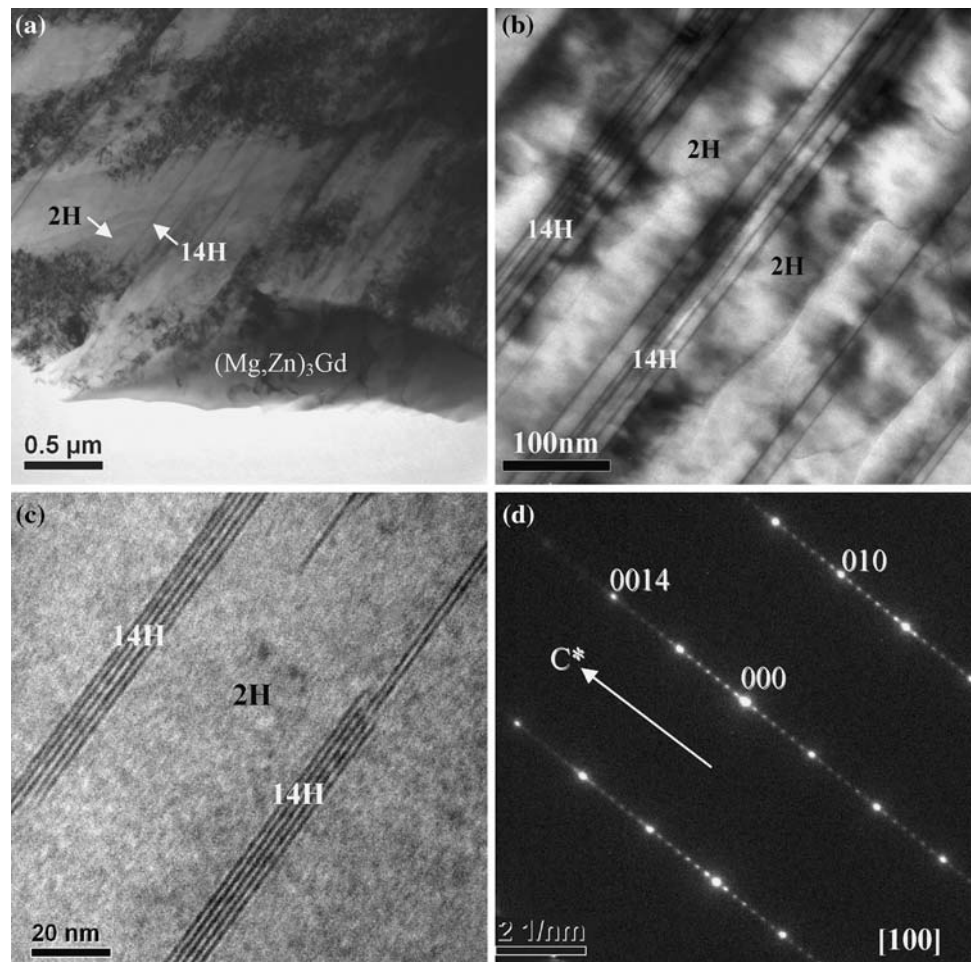
no LPSO structures in as-cast alloys but only after annealing at high temperatures (773 K) and annealing followed by aging treatment. Honma et al. [23] reported that the LPSO structure was formed in Mg-Gd-Y-Zn (-Zr) during the aging treatment at 488 K.

However, the coherent lamellae with the 14H-type LPSO structure have first been observed within  $\alpha'$ -Mg matrix in the as-cast Mg-Gd-Zn-Zr alloy produced by ingot metallurgy. In conclusion, microstructure of the as-cast  $\text{Mg}_{96.82}\text{Gd}_2\text{Zn}_1\text{Zr}_{0.18}$  alloy is mainly composed of  $\alpha'$ -Mg solid solution, and the coherent fine-lamellae consisting of the 2H-Mg and the 14H-type LPSO structure and the eutectic in which the second phase is the  $\beta$ -phase ( $(\text{Mg,Zn})_3\text{Gd}$ ).

Thereby, according to the results mentioned above in this study, what differ from their description [20–23] is concluded as follows: the lamellar 14H-type LPSO structure within  $\alpha'$ -Mg matrix is originally formed not by heat-treated (annealed and/or aging-treated) [20–24] but as-cast Mg-Gd-Zn (-Zr) alloys. Mg-Gd-Zn (-Zr) alloys are promising alloys for formation of the 14H-type LPSO



**Fig. 4** TEM observations for the lamellar 14H–LPSO structure within  $\alpha'$ -Mg matrix in the as-cast  $\text{Mg}_{96.82}\text{Gd}_2\text{Zn}_1\text{Zr}_{0.18}$  alloy. **a–c** BF images; **d** corresponding SAED pattern with the electron beam parallel to the  $[100]_z$  zone



structure in as-cast conditions, which are worthy of further study.

## Conclusions

Formation and characterization of the lamellar 14H-type LPSO structure within  $\alpha'$ -Mg matrix were investigated in the novel as-cast  $\text{Mg}_{96.82}\text{Gd}_2\text{Zn}_1\text{Zr}_{0.18}$  alloy. The conclusions are summarized as follows:

- (1) In the novel as-cast  $\text{Mg}_{96.82}\text{Gd}_2\text{Zn}_1\text{Zr}_{0.18}$  alloy produced by conventional ingot metallurgy, the microstructure is mainly composed of  $\alpha'$ -Mg solid solution, and the eutectic in which the second phase is the  $\beta$ -phase  $((\text{Mg,Zn})_3\text{Gd})$  and fine-lamellae. The fine-lamellae have first been observed within  $\alpha'$ -Mg matrix in as-cast Mg–Gd–Zn–Zr alloys.
- (2) The lamellae are composed of the 2H–Mg and the 14H-type LPSO structure. At present, the lamellar 14H-type LPSO structure within  $\alpha'$ -Mg matrix has first been observed in the as-cast Mg–Gd–Zn–Zr alloys. With respect to its initial formation condition,

it is not formed in heat-treated (annealed and/or aging-treated) but in as-cast Mg–Gd–Zn (–Zr) alloys.

- (3) The lamellae have coherent relationship, i.e.,  $(001)_{2\text{H-Mg}} // (0014)_{14\text{H-LPSO}}$  and  $[001]_{2\text{H-Mg}} // [001]_{14\text{H-LPSO}}$ . The lattice constants of the 2H–Mg and the 14H-type LPSO structure are estimated to be  $a = 0.325$  nm,  $c = 0.520$  nm and  $a = 0.325$  nm,  $c = 3.722$  nm, respectively. Their compositions are established to be Mg– $0.33 \pm 0.1$  at.% Zn– $0.57 \pm 0.1$  at.% Gd and Mg– $8.10 \pm 1.0$  at.% Zn– $11.05 \pm 1.0$  at.% Gd, respectively.

**Acknowledgements** Thanks are given to the support from the National Nature Science Foundation (50471015) and the SEM and TEM Laboratories of Analytical and Testing Center of Shanghai Jiaotong University.

## References

1. Peng QM, Hou XL, Wang LD et al (2009) Mater Des 30:292
2. Riontinoa G, Massazza M, Lussanaa D et al (2008) Mater Sci Eng A 494:445

3. Liu Y, Yuan GY, Lu C et al (2008) *J Mater Sci* 43:5527. doi: [10.1007/s10853-008-2839-4](https://doi.org/10.1007/s10853-008-2839-4)
4. Aghion E, Gueta Y, Moscovitch N et al (2008) *J Mater Sci* 43:4870. doi: [10.1007/s10853-008-2708-9](https://doi.org/10.1007/s10853-008-2708-9)
5. Lin L, Chen LJ, Liu Z (2008) *J Mater Sci* 43:4493. doi: [10.1007/s10853-008-2650-x](https://doi.org/10.1007/s10853-008-2650-x)
6. Gu ZH, Wang HY, Zheng N et al (2008) *J Mater Sci* 43:980. doi: [10.1007/s10853-007-2275-5](https://doi.org/10.1007/s10853-007-2275-5)
7. Tamura Y, Kida Y, Tamehiro H et al (2008) *J Mater Sci* 43:1249. doi: [10.1007/s10853-007-2276-4](https://doi.org/10.1007/s10853-007-2276-4)
8. Luo ZP, Zhang SQ (2000) *J Mater Sci Lett* 19:813
9. Kawamura Y, Hayashi K, Inoue A et al (2001) *Mater Trans* 42:1172
10. Inoue A, Kawamura Y, Matsushita M (2001) *J Mater Res* 16:1894
11. Abe E, Kawamura Y, Hayashi K et al (2002) *Acta Mater* 50:3845
12. Wang BS, Liu YB, An J (2008) *Mater Trans* 49:1768
13. Morikawa T, Kaneko K, Higashida K (2008) *Mater Trans* 49:1294
14. Itoi T, Seimiya T, Kawamura Y (2004) *Scr Mater* 51:107
15. Matsuda M, Ti S, Kawamura Y (2005) *Mater Sci Eng A* 393:269
16. Chen B, Lin DL, Zeng XQ et al (2007) *J Alloys Compd* 440:94
17. Kawamura Y, Morisaka T, Yamasaki M (2003) *Mater Sci Forum* 419–422:751
18. Amiya K, Ohsuna T, Inoue A (2003) *Mater Trans* 44:2151
19. Kawamura Y, Yamasaki M (2007) *Mater Trans* 48:2986
20. Yamasaki M, Anan T, Yoshimoto S (2005) *Scr Mater* 53:799
21. Yamasaki M, Sasaki M, Nishijima M et al (2007) *Acta Mater* 55:6798
22. Nishijima M, Hiraga K, Yamasaki M (2008) *Mater Trans* 49:227
23. Honma T, Ohkubo T, Kamado S et al (2007) *Acta Mater* 55:4137
24. Gao Y, Wang QD, Gu JH et al (2008) *J Alloys Compd*. doi: [10.1016/j.jallcom.2008.10.0003](https://doi.org/10.1016/j.jallcom.2008.10.0003)
25. Li JP, Yang Z, Liu T et al (2007) *Scr Mater* 56:137